Available online at www.sciencedirect.com

ScienceDirect

AASRI Procedia 6 (2014) 95 – 102

AASRI Procedia

www.elsevier.com/locate/procedia

2013 2nd AASRI Conference on Computational Intelligence and Bioinformatics

# A Simple Geometric Model for Simulating Brain Herniation Using CT Craniometry

Ke-Chun Huang[a], Furen Xiao[a,b], I-Jen Chiang[a,c], Yi-Long Chen[d], Yi-Hsin Tsai[a,e], Jau-Min Wong[a], Chun-Chih Liao[a,f]*

[a]*Institute of Biomedical Engineering, National Taiwan University, No.1, Sec.1, Ren'ai Rd., Taipei City 10051, Taiwan*
[b]*Clinical Center for Neuroscience, National Taiwan University Hospital, No.7, Zhongshan S. Rd., Taipei City 10002, Taiwan*
[c]*Graduate Institute of Medical Informatics, Taipei Medical University, No.250, Wuxing St., Taipei City 11031, Taiwan*
[d]*Institute of Biomedical Engineering, National Yang-Ming University, No.155, Sec.2, Linong St., Taipei City 11221, Taiwan*
[e]*Department of Surgery, Far Eastern Memorial Hospital, No.21, Sec.2, Nanya S. Rd., New Taipei City 22060, Taiwan*
[f]*Department of Neurosurgery, Taipei Hospital, No.127, Siyuan Rd., New Taipei City 24213, Taiwan*

**Abstract**

The intracranial space (ICS) is incompletely separated by the cerebral falx and the cerebellar tentorium into three compartments. To simulate brain herniation, defined as part of the brain shifting from one compartment to another, we proposed a simplified model of the supratentorial space (STS) based on computed tomographic (CT) images obtained from 50 subjects.

After identifying skull regions, we manually outlined the STS regions on CT slices. Pertinent dimensions of the STS and its openings were measured. The average volumes of the ICS and the STS were 1326 and 1154 mL. The average length, width and height of the STS were 154.7, 136.1, and 90.3 mm. The average length and height of the subfalcine space (SFS) were 85.8 and 52.1 mm, while the average length and width of midbrain were 37.9 and 30.9 mm.

Based on these data, we constructed a half sphere STS model with a diameter of 160 mm and a volume of 1072 mL. A 40 mm circle representing the tentorial incisura is removed from the center of its equatorial plane. This model is then divided into two compartments by its intact mid-sagittal plane, which had another 80 mm semicircle removed to simulate the SFS.

© 2014 The Authors. Published by Elsevier B. V. Open access under CC BY-NC-ND license.
Peer-review under responsibility of Scientific Committee of American Applied Science Research Institute

*Keywords: Brain herniation; Geometric model; Midline shift*

2212-6716 © 2014 The Authors. Published by Elsevier B. V. Open access under CC BY-NC-ND license.
Peer-review under responsibility of Scientific Committee of American Applied Science Research Institute
doi:10.1016/j.aasri.2014.05.014

## 1. Introduction

Lying within the cranial cavity, the human brain is composed of the cerebral hemispheres and the cerebellum, incompletely separated by the cerebral falx between the hemispheres and the cerebellar tentorium between the cerebrum and the cerebellum [1]. In other words, the intracranial space (ICS) is separated into the supratentorial space (STS) and the infratentorial space (ITS) by the tentorium. Because the brain is roughly bilateral symmetric, the falx is often used to represent the intact mid-sagittal plane (iMSP) and the separated cerebral hemispheres connect at the subfalcine space (SFS) [2]. The tentorial incisura (TI), an opening at the center of the tentorium, provides the only communication between the STS and the ITS [3]. The TI is divided into the anterior, middle, and posterior incisural spaces, with the midbrain (upper brainstem) occupying the middle one.

Different types of intracranial mass, such as hematomas, tumors, abscesses, or swelling brains after infarcts, can cause brain shift, followed by herniation, brainstem compression and death. With increased intracranial pressure (ICP), the diseased or injured cerebral hemisphere may herniate through the SFS to the other side, resulting in subfalcine herniation (SFH) which is manifested as midline shift (MLS) on brain images [4]. With bilateral cerebral lesions or further elevation of the ICP, the medial part of the cerebrum may herniate through the TI, resulting in transtentorial herniation (TTH) and brain stem compression. On images, one can find changes in the shape of the brainstem and effacement of the cisternal spaces around it [4]. Both types of cerebral herniation, SFH and TTH, are clinically and radiologically important phenomena that require special attention of physicians.

We have proposed methods that can automatically measure MLS with symmetry-based and landmark-based methods, and the results were verified clinically [5-8]. To our knowledge, however, there has been no biomechanical model dedicated to simulating brain herniation in the literature. In this study, we try develop a simple 3-dimensional geometric model that can be applied to simulate brain deformation, especially brain herniation occurring at the STS, caused by a supratentorial intracranial mass, based on computed tomographic (CT) images of patients with no intracranial pathologies.

## 2. Materials and Methods

### *2.1. Materials*

Compared to females, males have larger skulls and thus larger intracranial volumes (ICVs) [9, 10]. To create a generalized model, we collected computed tomographic (CT) images from 25 consecutive male and 25 consecutive female patients with brain concussion visiting the emergency room of Taipei Hospital, Department of Health, New Taipei City, Taiwan, between April and May in 2013. Patients with skull fractures, intracranial hematomas, history of neurological illnesses or intracranial surgeries, were excluded from this study.

All brain CT scans were done with a standard protocol using a Somatom Definition AS+ 128-slice scanner (Siemens, Erlangen, Germany). The field of view (FOV) was 250x250 mm. For patients with head injury only, contiguous 5-mm slices were obtained from the foramen magnum to the vertex with the gantry parallel to the orbitomeatal (OM) line. For those with concomitant facial and/or cervical spine injury, contiguous 5-mm slices were obtained from the neck to the vertex with the gantry perpendicular to the patient's couch.

Each CT image was 512x512 pixels in size, resulting in a resolution of 0.49 mm per pixel. To rule out the diagnosis of intracranial hematoma, the original CT density values were transformed from Hounsfield units to 8-bit gray values in a windowed value range (center 35 HU, width 150 HU) [6]. CT slices at levels from the

foramen magnum to the vertex were downloaded to a personal computer. All images were then inspected again by a board-certified neurosurgeon to confirm the absence of any exclusion criteria mentioned above.

### *2.2. Methods*

For each CT data set, the global gray level histogram was obtained. Then, pixels with bone density in all CT slices of the given data set were automatically tagged using a threshold derived from the histogram. The detailed settings were previously described [6, 7].

We have developed an algorithm that can differentiate the intracranial regions from the extracranial ones automatically [11]. With in the ICS, however, it is difficult to separate the STS from the ITS because the cerebellar tentorium is thin and has gray levels similar to the brain itself. Therefore, we manually labeled the boundary between the STS and the ITS and labeled the regions on the computer screen. The skull base openings of these regions were also labeled to prevent failures of the region-growing algorithm.

Using planimetry method of the Cavalieri principle, the volume of a given region is its area multiplied by the slice thickness. The total ICV, the volume of the STS (V_STS) and that of the ITS (V_ITS) of the patient, are the sum of the volumetric results of all corresponding regions across all CT slices. We also measured the length and width of the STS, defined as the largest anteroposterior diameter and the largest transverse diameter among all STS regions. The height of the STS is the total thickness of the STS volume, counted from the vertex to the level of the midbrain.

In addition to the volume and outer dimensions of the STS, we also measured the sizes of its openings, namely the SFS and the TI. The SFS and the TI meets at the midbrain. Due to the complex anatomy in this region, we only tried to identify the midbrain and omitted other structures such as vessels, nerves and the pituitary gland. The midbrains in the patients were manually recognized by human experts and their lengths and the widths were recorded. We measured its length of the SFS at the level of interventricular foramen of Monro [4]. We also counted the number of slices containing connected cerebral hemispheres from the corpus callosum down to the level of the midbrain and the total thickness was considered the height of the SFS.

## 3. Results

The ages of the patients ranged from 18 to 66 years with a mean of 37 ± 14 years. The mean ages of female and male patients were 39 ± 15 and 35 ±14 years, respectively.

### *3.1. Biometric Results*

Results of manual volumetry are listed in Table 1. The ICVs in the 50 patients ranged from 1040 to 1716 mL, with a mean of 1326 ± 138 mL. The V_STS ranged from 915 to 1480 mL with a mean of 1154 ± 119 mL, while the V_ITS ranged from 125 to 236 mL with a mean of 171 ± 23 mL. The ratio between V_STS and ICV had a small range from 0.85 to 0.89 with a mean of 0.87 ± 0.01. The volumes of all intracranial compartments were larger in males ($p < 0.001$, one-tail t-test). The volumes of the STS and the ITS are highly correlated, with a correlation coefficient of 0.777 ($p < 0.001$).

Table 1. Results of manual volumetry. The significance of the differences between females and males are given after each parameter.

| Pamameter | | Overall (n = 50) | Female (n = 25) | Male (n = 25) |
|---|---|---|---|---|
| ICV*** | Mean | 1326±138 | 1233±91 | 1419±112 |
| | Median | 1322 | 1228 | 1391 |
| | Range | 1040-1716 | 1040-1382 | 1264-1716 |

| | | | | |
|---|---|---|---|---|
| STS volume*** | Mean | 1154±119 | 1077±81 | 1232±100 |
| | Median | 1147 | 1074 | 1219 |
| | Range | 915-1480 | 915-1230 | 1096-1480 |
| ITS volume*** | Mean | 171±23 | 156±16 | 187±18 |
| | Median | 172 | 153 | 181 |
| | Range | 125-236 | 125-189 | 168-236 |

SD: standard deviation; ***: $p < 0.001$

Measurement results of outer and inner dimensions of the STS are listed in Table 2. The length of the STS in these 50 patients ranged from 138.7 to 175.8 mm with a mean of 153.7 ± 8.0 mm, while the width of the STS ranged from 116.7 to 150.9 mm with a mean of 136.1 ± 7.3 mm. The ratio between the length and the width of the STS ranged from 0.95 to 1.36 with a mean of 1.13 ± 0.09. The height of the STS ranged from 75.0 to 100.0 mm with a mean of 90.3 ± 4.5 mm. All outer dimensions of the STS were larger in males ($p = 0.010$ for the length, $p = 0.001$ for the width, and $p = 0.002$ for the height). The length/width ratio did not differ between males and females ($p=0.904$).

The length of the brainstem in these 50 patients ranged from 24.9 to 36.1 mm with a mean of 30.9 ± 2.5 mm, while the width of the brainstem ranged from 30.3 to 48.3 mm with a mean of 37.9 ± 4.7 mm. Compared to females, the length of the brainstem was larger in males, but the difference in brainstem width was only marginally significant ($p = 0.054$). The length of the SFS ranged from 67.8 to 103.9 mm with a mean of 85.8 ± 7.0 mm, while the height of the SFS ranged from 35.0 to 65.0 mm with a mean of 52.1 ± 5.7 mm. Males have larger SFS heights and lengths, but only the former showed significant difference ($p = 0.006$).

### *3.2. Model Specification*

Based on craniometric data from last section, we constructed a simple model of the STS. The model assumes the shape of the upper half of a sphere with a diameter of 160 mm. The volume of this STS model is 1072 mL, which is 6.7% smaller than the average V_STS but is very close to that of females, 1077 mL. Both the length and the width of this model are 160 mm. The length of the model is 3.9% larger than that of craniometry, while the width of the model is 17.6% larger. The height of the model, 80 mm, is 11% smaller than the average height of the STS obtained from craniometry.

The outer surface of this model simulates the convexity surfaces of the cerebral hemispheres. On the other hand, the irregular basal surface of the cerebrum, including the orbital roof, the sphenoid ridge, the middle cranial fossa floor and the tentorial surface, is simplified and represented by a flat equatorial plane in this model. A 40 mm circle is removed from the center of the basal plane to simulate the midbrain occupying the TI.

Table 2. Outer and inner dimensions of the STS. The significance of the differences between females and males are given after each parameter.

| Pamameter | | Overall (n = 50) | Female (n = 25) | Male (n = 25) |
|---|---|---|---|---|
| STS length* | Mean | 153.7±8.0 | 150.4±7.0 | 157.0±7.6 |
| | Median | 152.1 | 148.4 | 156.7 |
| | Range | 138.7-175.8 | 138.7-165.0 | 145.5 -175.8 |
| STS width** | Mean | 136.1±7.3 | 133.3±7.0 | 138.9±6.6 |
| | Median | 135.7 | 134.8 | 137.7 |
| | Range | 116.7-150.9 | 116.7-146.0 | 125.5-150.9 |
| STS height** | Mean | 90.3±4.5 | 88.6±4.5 | 92.0±3.8 |

| | | | | |
|---|---|---|---|---|
| | Median | 90.0 | 90.0 | 90.0 |
| | Range | 75.0-100.0 | 75.0-95.0 | 85.0-100.0 |
| Midbrain length*** | Mean | 30.9±2.5 | 29.6±2.3 | 32.1±2.1 |
| | Median | 30.7 | 30.3 | 32.2 |
| | Range | 24.9-36.1 | 24.9-33.7 | 28.3-36.1 |
| Midbrain width | Mean | 37.9±4.7 | 36.7±4.7 | 39.0±4.4 |
| | Median | 36.8 | 35.1 | 39.0 |
| | Range | 30.3-48.3 | 30.3-46.8 | 33.2-48.3 |
| SFS length | Mean | 85.8±7.0 | 84.0±7.4 | 87.7±6.2 |
| | Median | 87.4 | 84.9 | 88.8 |
| | Range | 67.8-103.9 | 67.8-103.9 | 74.7-97.6 |
| SFS height** | Mean | 52.1±5.7 | 50.4±6.1 | 53.8±4.8 |
| | Median | 55.0 | 50.0 | 55.0 |
| | Range | 35.0-65.0 | 35.0-60.0 | 45.0-65.0 |

SD: standard deviation; *: $p < 0.05$; **: $p < 0.01$; ***: $p < 0.001$

To model the partially connected cerebral hemispheres, our model is divided into two compartments by the iMSP. As a result, each cerebral "hemisphere", which assumes the shape of quarter sphere, has three surfaces: the convexity, the basal and the interhemispheric surfaces. The sickle-shaped falx cerebri is a strong arched process which descends vertically in the longitudinal fissure, or the iMSP [1]. It is narrow in front and broad behind. To model the falx, a semicircle 80 mm in diameter is removed from the iMSP to simulate the SFS. The center of this semicircle is located 20 mm anterior to the center of the basal plane. The posterior ends of SFS and the TI meet at the falcotentorial junction, which is adjacent to the posterior aspect of the midbrain.

We have implemented our model using ANSYS ED 10.0 (ANSYS, Inc., Canonsburg, PA) software environment. The cutaway view is shown in Fig. 1.

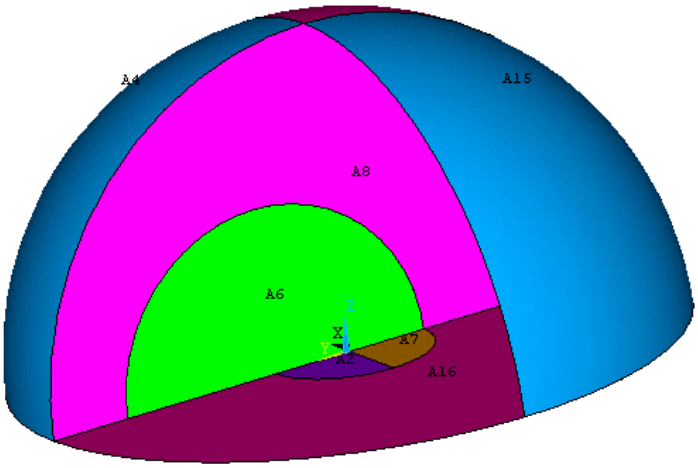


Fig. 1. Cutaway view of our model of the supratentorial brain. The X, Y, and Z axes of the Cartesian coordinate system refer to the right-left, anterior-posterior, and cranial-caudal (superior-inferior) anatomical axes, respectively. The left anterior quarter of the hemispheric object (A14) is removed to show the non-convexity surfaces. The interhemispheric surface is composed of the falx cerebri (A8) and the subfalcine space (A6). The basal surface is composed of the immobile part (A16) and the tentorial incisura (A2 and A7).

## 4. Discussion

### *4.1. Volumetry Results*

In this study, we performed measurements on the volumes and dimensions of the ICS. The ICVs obtained in our patient population seems smaller than those described in the literature (male: 1400-1600 mL, female: 1250-1450 mL) [9]. In addition to potential errors in the postprocessing process, partial volume effect caused by slice thickness may be the most important factor causing this discrepancy. Compared to the filling method, Sahin et al. had demonstrated a 3.7% underestimation of ICV using CT craniometry on dry skulls with 5-mm slices, probably due to partial volume effect [12, 13]. On the other hand, Sahin also noticed the systemic overestimating using 2-mm CT slices but the reason was unknown. This phenomenon may explain why studies using thin-cut slices or "volumetric" CT images may actually overestimate the ICV, such as the study done by Abbott et al. [14].

The ratio between V_ITS and ICV is important in patients with Chiari malformation type I. Using volumetric magnetic resonance imaging (MRI), Sgouros et al. measured these values in healthy and diseased pediatric subjects. In the healthy group, the ICV was 1383 mL, the V_ITS 186 mL and the PFV/ICV ratio was 0.135 [15]. In our study, the ratio between V_ITS and ICV ranged from 0.11 to 0.15 with an average of 0.13, which is very close to the normal value described by Sgouros.

We laboriously separated the STS regions from the ITS regions in this study. Lescot et al. also manually segmented the STS on 5-mm CT slices in 15 diseased and 15 healthy subjects [16]. They separated cerebrospinal fluid (CSF) voxels from brain voxels using thresholding. The average supratentorial brain volume of their healthy subjects was 1041 ± 108 mL, while the total intracranial CSF volume (V_CSF) was 127 ± 56 mL. The mean V_STS in current study (1154 mL) is compatible with Lescot's observation.

### *4.2. Model versus Reality*

Historiaclly, ICV estimation from craniometric parameters utilized the outer dimensions of the calvarial skull, A, B, and C, as well as its thickness, t. The ICV can then be calculated using the ellipsoid formula, ICV = pi / 6 * (A – 2t) (B – 2t) (C – 2t) [10]. In this study, we measured the inner dimensions of the skull directly on CT images. Since the thickness of the skull varied widely [17], we consider our method a better estimate because the ICV can be calculated directly.

In our simplified model of the STS, we did not take shape variation and sex difference into account. The outer and inner dimensions of the STS are simplified. The average length, width and height of the STS in our patients were 154.7, 136.1, and 90.3 mm. If we assuming that the STS is half ellipsoid in shape, the average V_STS would be 989 mL, considerably smaller than the actual volume of 1154 mL.

There are two reasons that can explain the underestimation caused by direct application of the ellipsoid formula. First, basal parts of the cerebral hemispheres are located below the level of the midbrain. In this study, about 13% of the V_STS was located caudal to the slice containing the midbrain and was not included in volumetry. Secondly, the largest lengths and widths of the STSs did not appear in the basal slice containing the TI (or the midbrain). Most of them were 20 mm, or 3-5 slices, above the basal slice. Direct application of the ellipsoid formula, which has the largest area at its equatorial plane, results in underestimation. On the other hand, with a length and width larger than the actual craniometry, our STS model can compensate for the underestimation of the volume.

Males have larger ICVs and V_STSs than females. Compare to females, the ICV was 15% larger, the V_STS 14% larger, the V_ITS 20% larger in males in this study. The average length, width, and height, as well as the inner dimensions, of the STS were about 4% larger in males. The model we created has a V_STS

close to that of females. To create a half sphere model that has a V_STS of the males, the diameter would be approximately 168 mm.

Theoretically, the CT studies produce a series of images that are parallel to the OM line. However, the actual gantry tilt angle varied from -2 to 28.2 degrees, depending on patient posture and whether there is need for cervical spine imaging. We did not find any relationship between the degree of gantry tilt and variables we measured (p=0.374). Sahin noted larger difference between volumetric results using coronal and axial slices of 10-mm thickness but the difference is small with 5-mm slices. [12]

The volumes of the STS and the ITS are highly correlated to that of ICV. Males have larger ICVs and thus larger V_STSs. In this study, all female patients have ICVs smaller than 1400 mL, while two male patients have ICVs larger than 1550 mL. Significant amount of extra-cerebral CSF exceeding 180 mL was observed in the patient with the largest ICV of 1716 mL, who had a ventricular CSF volume of 87 mL. On the other hand, smaller ventricles were observed in those with smaller ICVs. Since our model has a volume slightly smaller than the average V_STS of all male and female patients, we consider this model applicable to all patients except those with extremely large ICVs.

### *4.3. Potential applications*

The goal of this study is to develop a simple 3-dimensional geometric model of the STS that can be used in biomechanical simulations of brain herniation. Ideally, the cerebral hemispheres should fit tightly into both halves of the STS with minimal volume at the subdural and subarachnoid spaces. Under this condition, the dimensions of the cerebral hemispheres can be approximated by those of the STS model, obviating the need of creating another object to represent the skull. Boundary conditions, such as deformation or pressure loads, can be directly applied to our model. We can model SFH by immobilizing the falx cerebri (Area 8 in Fig. 1) while allowing brain movement at the SFS (Area 6). Similarly, we can model TTH by allowing free brain movement at the TI but limiting brain movement along the equatorial surface at other parts of the basal surface.

## 5. Conclusion

Based on CT craniometry, we have constructed a simple geometric model of the supratentorial space for simulating brain herniation. Having a volume close to that of a female adult, this model can be used in biomechanical studies.

## References

[1] H. Gray, and C. Clemente, Gray's Anatomy of the Human Body, 30 ed., Philadelphia, PA: Lippincott Williams & Wilkins, 1984.
[2] M. E. Brummer, “Hough transform detection of the longitudinal fissure in tomographic head images,” Medical Imaging, IEEE Transactions on, vol. 10, no. 1, pp. 74-81, 1991.
[3] A. L. Rhoton Jr, “Tentorial Incisura,” Neurosurgery, vol. 47, no. 3, pp. S131-S153, 2000.
[4] R. Bullock, R. Chesnut, J. Ghajar, D. Gordon, R. Hartl, D. Newell, F. Servadei, B. Walters, and J. Wilberger, “Appendix II: Evaluation of Relevant Computed Tomographic Scan Findings,” Neurosurgery, vol. 58, no. S2, p. 62, 2006.
[5] C. C. Liao, I. J. Chiang, F. Xiao, and J. M. Wong, “Tracing the Deformed Midline on Brain CT,” Biomedical Engineering: Applications, Basis and Communications, vol. 18, no. 06, pp. 305-311, 2006.
[6] C. C. Liao, F. R. Xiao, J. M. Wong, and I. J. Chiang, “Automatic recognition of midline shift on brain CT

images," Computers in Biology and Medicine, vol. 40, no. 3, pp. 331-339, Mar, 2010.
[7] F. R. Xiao, I. J. Chiang, J. M. Wong, Y. H. Tsai, K. C. Huang, and C. C. Liao, "Automatic measurement of midline shift on deformed brains using multiresolution binary level set method and Hough transform," Computers in Biology and Medicine, vol. 41, no. 9, pp. 756-762, Sep, 2011.
[8] F. Xiao, C. C. Liao, K. C. Huang, I. J. Chiang, and J. M. Wong, "Automated assessment of midline shift in head injury patients," Clin Neurol Neurosurg, vol. 112, no. 9, pp. 785-90, Nov, 2010.
[9] B. Sahin, "Handbook of Anthropometry: Physical Measures of Human Form in Health and Disease," V. R. Preedy, ed., Springer, 2012.
[10] A. S. Dekaban, "Tables of cranial and orbital measurements, cranial volume, and derived indexes in males and females from 7 days to 20 years of age," Annals of Neurology, vol. 2, no. 6, pp. 485-491, 1977.
[11] C. C. Liao, F. Xiao, J. M. Wong, and I. J. Chiang, "Computer-aided diagnosis of intracranial hematoma with brain deformation on computed tomography," Computerized Medical Imaging and Graphics, vol. 34, no. 7, pp. 563-571, 2010.
[12] B. Sahin, M. Mazonakis, H. Akan, S. Kaplan, and Y. Bek, "Dependence of computed tomography volume measurements upon section thickness: An application to human dry skulls," Clinical Anatomy, vol. 21, no. 6, pp. 479-485, 2008.
[13] T. H. Grumme, W. Kluge, K. Kretzschar, and A. Roesler, Cerebral and spinal computed tomography, Berlin: Blackwell Wissenschafts-Verlag, 1998.
[14] A. H. Abbott, D. J. Netherway, D. B. Niemann, B. Clark, M. Yamamoto, J. Cole, A. Hanieh, M. H. Moore, and D. J. David, "CT-Determined Intracranial Volume for a Normal Population," Journal of Craniofacial Surgery, vol. 11, no. 3, pp. 211-223, 2000.
[15] S. Sgouros, M. Kountouri, and K. Natarajan, "Posterior fossa volume in children with Chiari malformation Type I," Journal of Neurosurgery: Pediatrics, vol. 105, no. 2, pp. 101-106, 2006.
[16] T. Lescot, M. P. Bonnet, A. Zouaoui, J. C. Muller, C. Fetita, P. Coriat, and L. Puybasset, "A quantitative computed tomography assessment of brain weight, volume, and specific gravity in severe head trauma," Intensive Care Medicine, vol. 31, no. 8, pp. 1042-1050, 2005.
[17] F. Xiao, I. J. Chiang, T. M. Hsieh, K. C. Huang, Y. H. Tsai, J. M. Wong, H. W. Ting, and C. C. Liao, "Estimating postoperative skull defect volume from CT images using the ABC method," clinical neurology and neurosurgery, vol. 114, pp. 205-10, 2012.